Supplemental Files – Souders and Sylvester

Appendix A1.
Method – Thermal Ionization Mass Spectrometry (TIMS)

Feldspar minerals and sulfides chosen for thermal ionization mass spectrometry (TIMS) analysis were in the form of coarse solid fragments prior to dissolution with the exception of USGS MASS-1, which was a powder. All TIMS analytical work was performed in the Boise State University Isotope Geology Laboratory (IGL). For the feldspar minerals, each individual sample was between ~0.003 and 0.01g. Prior to dissolution, any potential surface contamination was removed from the feldspar separates through a series of steps. First, 1 mL of 3.5 N HNO_3 was added to each sample, the sample capped and placed on a hot plate at 120 C for ~30 minutes. The HNO_3 was then removed with a pipette and each sample was rinsed three-times with milli-Q H_2O. 1 mL of 6M HCl was then added to each sample and again each sample was capped and placed on a hotplate set at 120 C. After ~30 minutes, the HCl was removed with a pipette and each feldspar separate was rinsed three-times with 0.5 mL milli-Q H_2O. Following the milli-Q H_2O rinse, a mixture of 1 mL concentrated (16M) HNO_3 and 3 mL concentrated (29M) HF was added to each sample. Each feldspar sample was then capped and placed on a hotplate set at ~150 C overnight. For the solid sulfide samples PB-1 and B41, 0.004 to 0.015 g chunks were dissolved in a mixture of 0.5 mL concentrated (16M) HNO_3 and 0.2 mL concentrated (16M) HCl mixture overnight on a hotplate set at ~150 C. Prior to dissolution, each sulfide solid was rinsed three-times with milli-Q H_2O and sonicated in milli-Q H_2O for 10 minutes to remove any surface contamination. For MASS-1, the sulfide powder, ~ 0.01 g of power was dissolved in a mixture of 3 mL concentrated (16M) HNO_3 and 1 mL concentrated (16M) HCl and fluxed on a hotplate at ~150 C overnight.

After one night fluxing on a hotplate at ~150 C, all samples were fully dissolved in their respective acid mixtures. Each sample beaker was then uncapped and placed back on a hotplate under a heat lamp until dry. Once dry, 1 mL of concentrated (16M) HCl was added to each sample. Capped samples were then sonicated for ~1 hour. An additional 4 mL of 6M HCl (feldspar samples and MASS-1) or 1 mL of 6M HCl (PB-1 and B41) was added to each sample, the beakers capped and each sample was again placed back on a hotplate set at ~120 C to flux overnight. After ~24 hours on a hotplate, all samples were fully dissolved in 6M HCl. Each sample beaker was uncapped and the samples dried down to salts on a hotplate.

Both feldspar and sulfide samples were and then converted to $PbBr_4^{2-}$ by adding 1 mL 0.5M HBr to each sample and placing on the hot plate until dry. Prior to ion exchange chromatography, each sample was redissolved in 1 mL of 0.5M HBr. Lead was separated from each matrix using ion-exchange columns filled with 100 μL (resin volume) AG1-X8, 200-400 mesh, and HCl-based anion exchange chromatography procedures.

Lead was analyzed on the Isoprobe-T thermal ionization mass spectrometer. Lead was loaded on single Re filaments with 1 – 2 μL of a dilute silica gel – 0.1M H_3PO_4 emitter solution. Lead was measured in static mode, maintaining a 3V ^{208}Pb beam for 200 cycles, or, for very small amounts of lead, dynamically peak-switching all ion beams into the Daly detector. TIMS lead isotope ratio results for the feldspars and sulfide minerals adopted for this study are listed in Table A2.

Appendix A2.
Sample Characterization/Description

Prior to analysis, small separates (≤ 1 mm in thickness and no greater than 5 mm in any surface direction) of all silicate glasses, feldspars and sulfides were mounted in 10 mm or 25 mm diameter epoxy resin mounts and once cured, ground down to a flat surface and polished using diamond abrasive to expose a cross-sectional surface of each material. Sulfides and silicates were placed in separate epoxy mounts and the sulfides were polished on polishing cloths specifically designated for sulfide minerals.

The Shap orthoclase has been used in several other investigations[1,2] as a secondary standard due to its homogeneous lead isotope composition on the μm-scale of a laser ablation analysis[3]. The Fish Canyon Tuff (FCT) sanidine has been analyzed for trace element concentrations, including lead, by Bachmann et al.[4]. TIMS lead isotope ratio values for the FCT sanidine adopted for this study are those determined by Hemming and Rasbury[5]. The bulk compositions of all three feldspars are given in Table A3.

Three different synthetic sulfides were analyzed as part of this investigation. Bulk analyses of

the three sulfides are presented in Table A4. Surface images highlighting the differences in physical character of the 3 sulfides analyzed are presented in Figure A2.1.

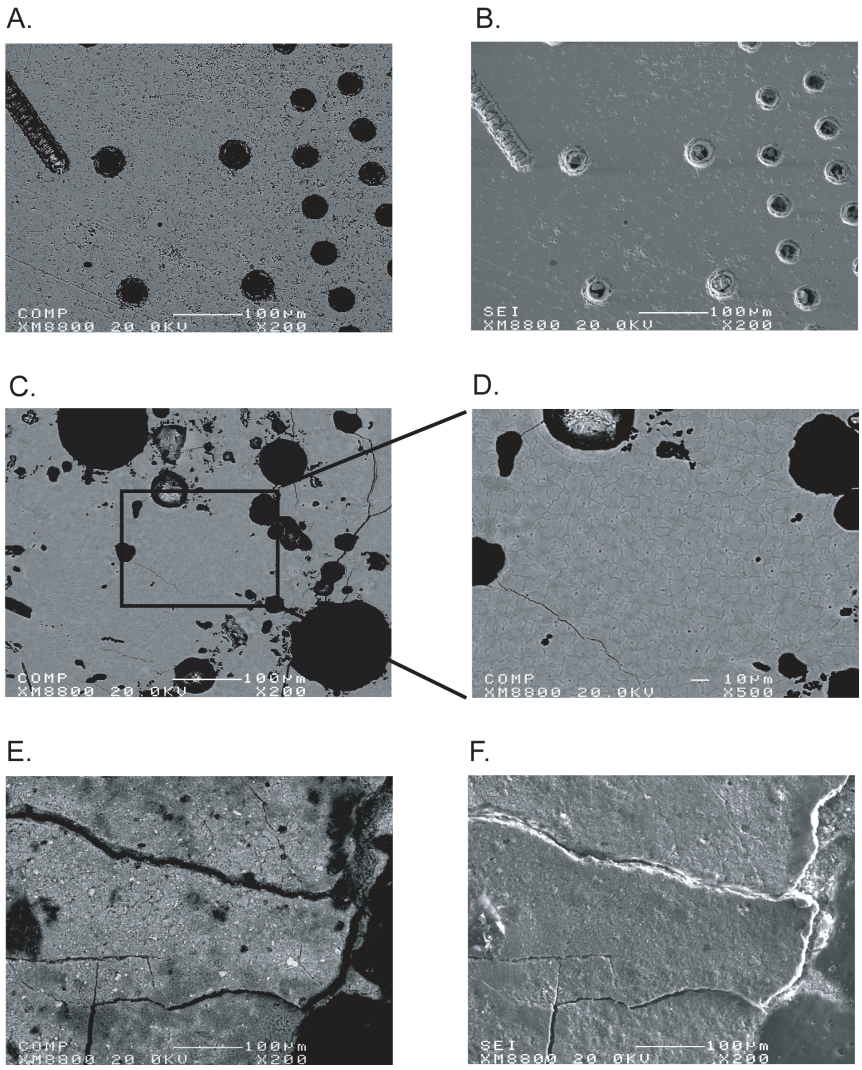

Figure A2.1 (A) Back-scattered electron (BSE) and (B) Secondary electron (SE) images of the same surface area of sulfide glass, PB-1. 30 – 40 µm diameter laser ablation pits and line scans mark the surface of the sulfide. (C and D) BSE images of sulfide sinter B-41 taken at two different magnifications. The area within the box in C is image D. The subtle changes in the gray-scale best seen in image D most likely are the result of individual grains approaching their melting points. (E) BSE and (F) SE images of the same surface area of pressed powder pellet MASS-1. Individual grains of different compositions can be readily identified in the BSE image by the varying levels of brightness. All images were collected on the JXA JEOL-8900L superprobe at McGill University.

Appendix A3.

Ablation Rate Determination Procedures

Ablation rates were calculated by dividing the surface to depth distance (μm) of a laser ablation crater by the ablation time to produce the crater (seconds). Representative craters for each matrix were drilled under ablation conditions identical to those used for each experiment. In order to monitor changes in pit morphology during the laser ablation interval, representative craters were produced for 10 seconds, 30 seconds and 60 seconds of laser ablation (3 different craters/matrix/set of ablation conditions). Secondary electron (SE) images of each crater were taken using a FEI Quanta 400 environmental secondary electron microscope (SEM) with an accelerating voltage of 15 kV and a beam diameter of 3.14 μm.

The surface to depth distance was determined in a series of steps (Figure A3.1). First, a SE image of the crater was taken to identify major physical features on the floor and walls of the pit. The SEM stage was then tilted to a 35 degree angle and a second SE image of the same crater was taken, making sure the SEM working distance (~20 mm) remained constant. Once distinguishing morphological features on the floor and walls of the crater had been identified, the tilt on the SEM stage was adjusted until the near-side crater rim was in line with the intersection of the crater floor and far-side crater wall (Figure A3.2). The tilt angle of the SEM stage was recorded and a third SE image was taken. After the proper tilt angle of the SEM stage was determined, the distance between the near-side crater rim and the crater wall/crater floor intersection point was measured directly from the 'in-line' tilted SE crater image. The surface to depth distance was calculated using the formula:

$$h = w * \tan(90 - \theta)$$

where: h = surface to depth distance
w = crater width measured from 'in-line' tilted image
θ = tilt angle of the SEM stage for 'in-line' image

The apparent drill rates calculated are a function of how fast the laser is drilling down into a matrix over a given period of time and how much material is excavated from the crater within the same time interval. Our method also assumes both the sample surface and crater floor

intersect the crater walls at right angles and the surface pit width equals the pit width on the crater floor. Determining the crater depth from sample surface to crater floor is critical when calculating drill rates, yet this quantitative measurement is obscured by melt deposition along the crater rim extending above the sample surface, and the build-up of melt droplet piles on the crater floor. The crater depth calculation assumes each crater is a cylinder, with a top and bottom of equal diameter and straight sides. This method does not account for tapering of the crater walls. Although variations exist between matrices, the estimate of the error on our apparent drill rate calculations does not exceed 20% of the calculated ablation rate. For example, if a 2 μm tall rim is associated with each ablation pit, the crater depth would decrease up to 11 % and there would be up to an 11% decrease in calculated drill rates. If we assume an ~8 μm high melt droplet pile on each crater floor, the crater depth would increase by up to 20 %. This translates to an ~20 % increase in the drill rates calculated. It is important to note when considering the potential errors on the apparent drill rate calculations that the difference in drill rates between the ~30 μm diameter craters and the ~69 μm diameter craters are still distinct.

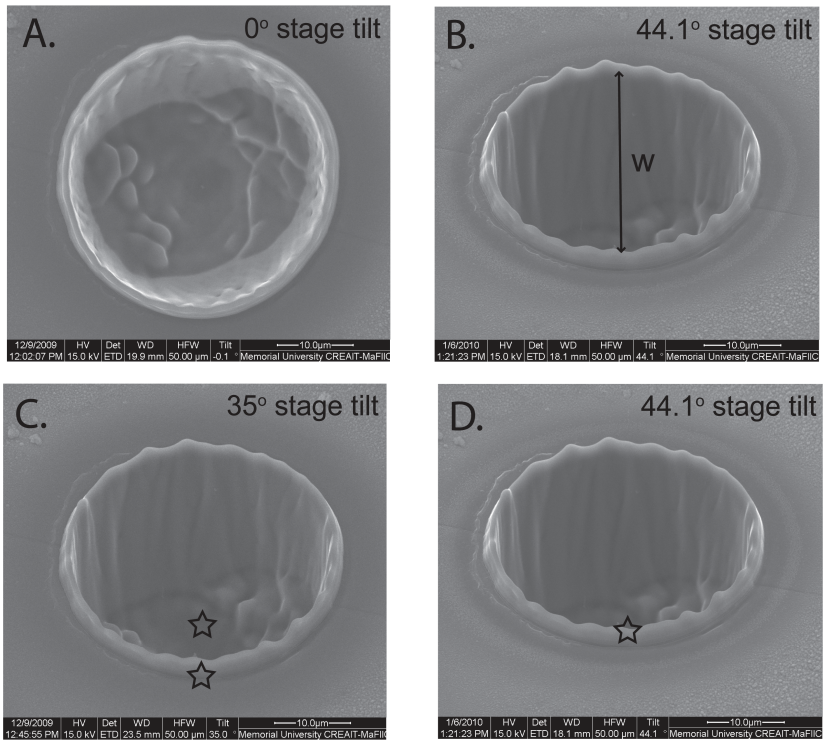

Figure A3.1. Secondary electron (SE) crater images. (A) Initial SE image taken to aid in the identification of major morphological features inside the crater. (B) Distance measured on 'in-line' tilt image to determine crater width (w). (C) Thirty-five degree stage-tilt SE image. The near-side crater rim and the intersection of the crater floor and far-side crater wall are marked with stars. (D) 'In-line' SE tilt image. The star marks where the near-side crater rim and the intersection of the crater floor and far-side crater wall are lined up.

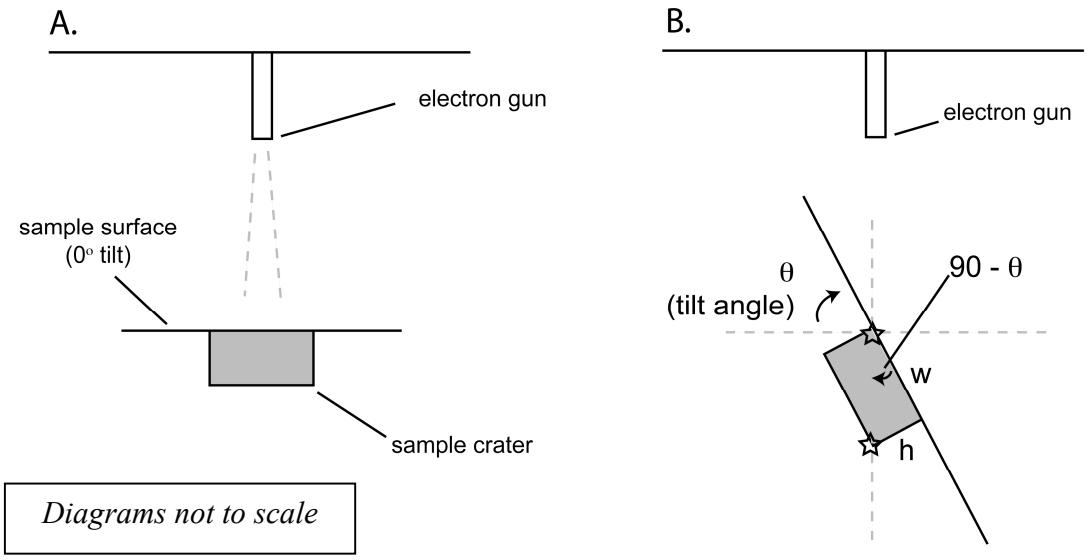

Figure A3.2. Schematic cross-section of the SEM chamber with (A) the stage at 0° tilt and (B) the stage tilted to an angle (θ) where the near-side crater rim and the intersection of the crater floor and far-side crater wall are in-line. Both the near-side crater rim and the intersection of the crater floor with the far-side crater wall are marked with stars. The crater width (w) and surface to depth distance (h) are also labeled. Both diagrams are not to scale.

References

1 P.D. Clift, H. Van Long, R. Hinton, R.M. Ellam, R. Hannigan, M.T. Tan, J. Blusztajn, N.A. Duc, 2008, *Geochem. Geophys. Geosyst.*, **9**, Q04039, DOI:10.1029/2007GC001867.

2 S. Tyrrell, S. Leleu, A.K. Souders, P.D.W. Haughton, J.S. Daly, 2009, *Geol. J.*, **44**, 692-710.

3 S. Tyrrell, P.D.W. Haughton, J.S. Daly, T.F. Kokfelt, D. Gagnevin, *J. Sed. Res.*, 2006, **76**, 324 – 345.

4 O. Bachmann, M.A. Dungan, F. Bussy, 2005, *Contrib. Mineral. Petrol.*, **149**, 338-349.

5 S.R. Hemming, E.T. Rasbury, 2000, *Chem. Geol.*, **165**, 331-337.

6 GeoReM, Max-Planck-Institute data base for geological and environmental reference materials, http://georem.mpch-mainz.gwdg.de/

7 J. Baker, S. Stos, T. Waight, *Archaeometry*, 2006, **48**, 45 – 56.

8 S.A. Wilson, W.I. Ridley, A.E. Koenig, 2002, *J. Anal. At. Spectrom.*, **17**, 4006-4009.

Supplemental Files – Souders and Sylvester

Table A1. Calibration values for silicate glasses used for LA-MC-ICPMS lead isotope analysis

Sample	^{206}Pb / ^{204}Pb	2SD	^{207}Pb / ^{204}Pb	2SD	^{208}Pb / ^{204}Pb	2SD	^{207}Pb / ^{206}Pb	2SD	^{208}Pb / ^{206}Pb	2SD	refernce
BCR2-G	18.765	0.014	15.626	0.012	38.73	0.04	0.833	0.002	2.066	0.002	GeoREM preferred
NIST 612	17.099	0.003	15.516	0.002	37.02	0.007	0.90745	0.0017	2.1651	0.001	Baker et al. (2004)
NIST 614	17.842	0.01	15.541	0.001	37.499	0.009	0.87101	0.0004	2.1017	0.001	Baker et al. (2004)

Table A2. Thermal Ionization Mass Spectrometry (TIMS) Pb isotope ratios for the sulfide and feldspars analyzed and/or included in this investigation.

Sample		$^{206}Pb/^{204}Pb$ [1]	$\%\sigma_m$ [2]	$^{207}Pb/^{204}Pb$ [1]	$\%\sigma_m$ [2]	$^{208}Pb/^{204}Pb$ [1]	$\%\sigma_m$ [2]	$^{207}Pb/^{206}Pb$ [1]	$\%\sigma_m$ [2]	$^{208}Pb/^{206}Pb$ [1]	$\%\sigma_m$ [2]
PB-1-1	sulfide glass	20.606	0.002	15.839	0.003	39.607	0.003	0.76869	0.0006	1.9221	0.0010
PB-1-2	sulfide glass	20.546	0.002	15.829	0.002	39.533	0.002	0.77043	0.0005	1.9241	0.0007
PB-1-3	sulfide glass	20.606	0.003	15.832	0.003	39.536	0.003	0.76831	0.0006	1.9186	0.0010
	AVERAGE	20.586		15.834		39.559		0.769		1.922	
	SD (1s)	0.0346		0.0052		0.0419		0.0011		0.0028	
	%RSD (1s)	0.17%		0.03%		0.11%		0.15%		0.14%	
Mass1-A	pressed powder	20.000	0.006	15.771	0.006	39.118	0.007	0.7887	0.0010	1.9561	0.0017
Mass1-B	pressed powder	20.443	0.005	15.810	0.005	39.477	0.005	0.7734	0.0007	1.9311	0.0012
Mass1-C	pressed powder	20.509	0.004	15.825	0.004	39.553	0.005	0.7716	0.0007	1.9286	0.0012
	AVERAGE	20.317		15.802		39.383		0.778		1.939	
	SD (1s)	0.2772		0.0278		0.2322		0.0094		0.0152	
	%RSD (1s)	1.36%		0.18%		0.59%		1.20%		0.78%	
B41 A	sulfide sinter	18.623	0.004	15.678	0.004	38.209	0.004	0.8419	0.0007	2.0518	0.0006
B41 B	sulfide sinter	18.461	0.010	15.672	0.011	38.094	0.011	0.8489	0.0013	2.0635	0.0022
B41 C	sulfide sinter	18.613	0.003	15.678	0.003	38.202	0.003	0.8423	0.0008	2.0524	0.0008
	AVERAGE	18.566		15.676		38.168		0.844		2.056	
	SD (1s)	0.0907		0.0035		0.0642		0.0040		0.0066	
	%RSD (1s)	0.02%		0.02%		0.17%		0.47%		0.32%	
SHAP A (lg)	orthoclase	18.267	0.001	15.662	0.001	38.281	0.001	0.8574	0.0003	2.0956	0.0005
SHAP B	orthoclase	18.272	0.002	15.649	0.002	38.236	0.002	0.8565	0.0004	2.0926	0.0005
SHAP C	orthoclase	18.243	0.002	15.649	0.002	38.240	0.002	0.8578	0.0004	2.0961	0.0005
SHAP D	orthoclase	18.302	0.002	15.662	0.002	38.276	0.002	0.8558	0.0004	2.0913	0.0004
	AVERAGE	18.271		15.656		38.258		0.857		2.094	
	SD (1s)	0.0242		0.0074		0.0236		0.0009		0.0023	
	%RSD (1s)	0.13%		0.05%		0.06%		0.11%		0.11%	
159430 (lg)	bytownite	13.308	0.001	14.442	0.001	33.074	0.001	1.0852	0.0003	2.4854	0.0003
159430 A	bytownite	13.246	0.015	14.441	0.015	33.060	0.015	1.0902	0.0018	2.4959	0.0018
159430B	bytownite	13.272	0.010	14.490	0.010	33.173	0.011	1.0919	0.0050	2.4999	0.0049
	AVERAGE	13.275		14.457		33.103		1.089		2.494	
	SD (1s)	0.0308		0.0281		0.0612		0.0035		0.0075	
	%RSD (1s)	0.23%		0.19%		0.19%		0.32%		0.30%	
Fish Canyon Sanidine(10 gr, 1.3 mg) [3]		18.483	0.043	15.617	0.051	37.865	0.066	0.8449	0.0007	2.0486	0.0008
Fish Canyon Sanidine(10 gr, 2.1 mg) [3]		18.461	0.010	15.591	0.016	37.74	0.018	0.8445	0.0002	2.0443	0.0002
	AVERAGE	18.472		15.604		37.8025		0.8447		2.0465	
	SD (1s)	0.016		0.018		0.088		0.000		0.003	
	%RSD (1s)	0.08%		0.12%		0.23%		0.03%		0.15%	

1 - ratios reported fractionation corrected 0.11%/amu based upon repeated measurements of NBS-981, NBS-982 and BCR-1

2 - $\%\sigma_M$ is internal relative 1-sigma standard error; fractionation uncertainty imposes the following conservative absolute uncertainties (1-sigma): 208Pb/204Pb, 0.019; 207Pb/204Pb, 0.007; 206Pb/204Pb, 0.008; 208Pb/206Pb, 0.0009; 207Pb/206Pb, 0.0004

3 - Pb isotope ratios from Hemming and Rasbury (2000).

Supplemental Files – Souders and Sylvester

TABLE A3. Major element composition and lead concentration of feldspars analyzed.

SAMPLE	METHOD		SiO2 wt (%)	Al2O3 wt (%)	FeO wt (%)	MgO wt (%)	CaO wt (%)	Na2O wt (%)	K2O wt (%)	BaO wt (%)	Cl wt (%)	Total	Pb [2] ppm
Shap orthoclase	EMP[1]	Average (n=10)	64.82	18.56	0.08	0.01	0.05	1.61	14.24	0.34	< LD	99.70	~35
		Stdev	0.337	0.113	0.020	0.007	0.045	0.786	1.168	0.155			
Fisken¾sset bytownite	EMP[1]	Average (n=24)	46.74	33.81	0.11	N/A	17.27	1.82	0.04	< LD	0.08	99.88	~6.25
		Stdev	1.185	0.719	0.019		0.823	0.473	0.017		0.046		
FCT sanidine	EMP[1]	Average (n=12)	64.78	18.75	0.11	< LD	0.17	2.65	12.46	0.78	< LD	99.69	~20
		Stdev	0.534	0.149	0.024		0.014	0.079	0.155	0.438			

< LD: below detection limits

[1] EMP data for feldspars collected on the JXA JEOL-8900L superprobe at McGill University with an accelerating voltage of 15 kV, beam current of 20 nA, using a 5 um beam and a 20 second counting time for each element of interest.

[2] Shap orthoclase total Pb concentration fromTyrrell et al. (2006) and average FCT sanidine total Pb concentration from Bachmann et al. (2005)

TABLE A4. Major element composition and Pb concentration of sulfides analyzed.

SAMPLE	METHOD		Zn wt (%)	Ni wt (%)	S wt (%)	Fe wt (%)	Co wt (%)	Cu wt (%)	Pb[1] (ppm)
PB-1	EMP[2]	Average (n=22)	-	4.897	37.475	57.046	-	-	19.417
		Stdev	-	0.0458	0.1788	0.2114	-	-	
B41	EMP[2]	Average (n=24)	-	6.894	36.870	51.094	-	4.706	15.788
		Stdev	-	0.8465	0.5881	1.9370	-	3.3423	
MASS-1	various[3]		21	-	27.6	15.6	67	13.4	
	solution - ICPMS[4]		18.74	-	-	11.799	-	13.636	67.273

[1] Pb concentration determined by solution ICP-MS at Memorial University

[2] EMP data for PB-1 and B41 collected on the JXA JEOL-8900L superprobe at McGill University with an accelerating voltage of 20 kV, beam current of 30 nA, using a3 um beam and a 20 second counting time for each element of interest.

[3] Zn, Fe, Cu determined by electron microprobe (EM), solution ICPMS, and ICP atomic emission spectrometry; Co analyzed by solution ICPMS and instrumental neutron activation analysis (INAA); S determined by cumbustion infared spectroscopy (CIS) (Wilson et al. 2002)

[4] average values determined by solution ICP-MS at Memorial University and Charles University

Table A5 Supplementary Data: LA-MC-ICPMS lead isotope ratios for three feldspar matrices (Souders and Sylvester, 2010)

Sample	Analysis ID	Std	^{206}Pb / ^{204}Pb	std error (1-sigma)	^{207}Pb / ^{204}Pb	std error (1-sigma)	$^{208}Pb/^{204}Pb$	std error (1-sigma)	$^{207}Pb/^{206}Pb$	std error (1-sigma)	$^{208}Pb/^{206}Pb$	std error (1-sigma)
Shap orthoclase	oc13b16	BCR2G	18.334	0.095	15.719	0.092	38.141	0.292	0.860	0.002	2.085	0.006
Shap orthoclase	oc13b17	BCR2G	18.215	0.102	15.615	0.096	38.010	0.300	0.859	0.002	2.095	0.005
Shap orthoclase	oc13b18	BCR2G	18.294	0.097	15.658	0.092	38.329	0.293	0.859	0.002	2.099	0.006
Shap orthoclase	my01b12	BCR2G	18.192	0.138	15.649	0.099	38.277	0.214	0.860	0.003	2.101	0.005
Shap orthoclase	my01b24	BCR2G	18.254	0.167	15.606	0.125	38.122	0.291	0.858	0.003	2.096	0.005
Shap orthoclase	my01c05	BCR2G	18.242	0.182	15.719	0.145	38.315	0.376	0.860	0.002	2.096	0.004
Shap orthoclase	my01c12	BCR2G	18.263	0.237	15.748	0.202	38.183	0.465	0.857	0.003	2.099	0.006
Shap orthoclase	my01d05	BCR2G	18.285	0.120	15.711	0.109	38.426	0.266	0.859	0.003	2.101	0.007
Shap orthoclase	my01d12	BCR2G	18.388	0.128	15.787	0.117	38.466	0.281	0.858	0.003	2.093	0.007
Shap orthoclase	my01e05	BCR2G	18.293	0.137	15.617	0.124	38.390	0.320	0.859	0.002	2.100	0.005
Shap orthoclase	my01e12	BCR2G	18.127	0.119	15.487	0.114	38.135	0.290	0.854	0.002	2.093	0.005
Shap orthoclase	my01f05	BCR2G	18.322	0.204	15.687	0.203	38.267	0.475	0.856	0.003	2.097	0.006
Shap orthoclase	my01g12	BCR2G	18.229	0.158	15.653	0.143	38.170	0.313	0.861	0.003	2.103	0.008
Shap orthoclase	my02b05	BCR2G	18.265	0.069	15.659	0.070	38.299	0.161	0.859	0.001	2.102	0.003
Shap orthoclase	my02b12	BCR2G	18.311	0.088	15.749	0.086	38.314	0.194	0.861	0.002	2.103	0.003
Shap orthoclase	oc13d19	612	18.282	0.051	15.685	0.047	38.519	0.140	0.858	0.001	2.103	0.004
Shap orthoclase	oc13d20	612	18.237	0.064	15.600	0.061	38.234	0.171	0.856	0.001	2.098	0.003
Shap orthoclase	oc13d21	612	18.247	0.069	15.669	0.069	38.342	0.167	0.860	0.001	2.098	0.003
Shap orthoclase	my01a04	612	18.407	0.110	15.764	0.082	38.601	0.248	0.857	0.002	2.100	0.005
Shap orthoclase	my02c12	612	18.276	0.071	15.731	0.064	38.340	0.143	0.859	0.002	2.095	0.003
Shap orthoclase	my02d04	612	18.221	0.074	15.616	0.073	38.086	0.166	0.857	0.002	2.091	0.003
Shap orthoclase	my02d12	612	18.337	0.068	15.751	0.064	38.421	0.121	0.861	0.002	2.098	0.002
Shap orthoclase	my02e04	612	18.300	0.079	15.672	0.064	38.297	0.155	0.857	0.002	2.095	0.003
Shap orthoclase	my02e12	612	18.379	0.068	15.771	0.060	38.581	0.144	0.857	0.002	2.099	0.003
Shap orthoclase	my02e24	612	18.338	0.077	15.760	0.076	38.355	0.181	0.857	0.002	2.090	0.004
Shap orthoclase	my02f04	612	18.322	0.082	15.697	0.070	38.343	0.173	0.857	0.001	2.096	0.003
Shap orthoclase	my02f12	612	18.201	0.094	15.578	0.071	38.088	0.202	0.857	0.001	2.089	0.003
Shap orthoclase	my02g04	612	18.246	0.085	15.618	0.090	38.231	0.216	0.858	0.001	2.094	0.004
Shap orthoclase	my02g12	612	18.257	0.061	15.690	0.065	38.332	0.178	0.858	0.001	2.098	0.004
Shap orthoclase	my02h04	612	18.337	0.095	15.722	0.070	38.284	0.204	0.857	0.002	2.092	0.004
FCT sanidine	oc05a10	BCR2G	18.481	0.145	15.595	0.144	37.945	0.319	0.844	0.002	2.050	0.005
FCT sanidine	oc05a11	BCR2G	18.464	0.138	15.547	0.139	37.847	0.306	0.844	0.002	2.053	0.005
FCT sanidine	oc05a12	BCR2G	18.476	0.134	15.527	0.138	37.913	0.303	0.842	0.002	2.052	0.005
FCT sanidine	oc05a16	BCR2G	18.434	0.139	15.548	0.140	37.842	0.304	0.845	0.002	2.051	0.004
FCT sanidine	oc05a17	BCR2G	18.477	0.137	15.646	0.142	38.003	0.307	0.847	0.002	2.054	0.004
FCT sanidine	oc05a18	BCR2G	18.489	0.140	15.633	0.142	37.987	0.311	0.845	0.002	2.048	0.004
FCT sanidine	oc05a23	BCR2G	18.506	0.142	15.540	0.143	37.960	0.310	0.844	0.002	2.046	0.005
FCT sanidine	oc05a24	BCR2G	18.452	0.146	15.550	0.144	37.860	0.318	0.844	0.002	2.045	0.005
FCT sanidine	oc13b10	BCR2G	18.440	0.109	15.703	0.116	37.915	0.312	0.849	0.003	2.047	0.007
FCT sanidine	oc13b11	BCR2G	18.469	0.176	15.695	0.166	37.804	0.436	0.848	0.003	2.050	0.006
FCT sanidine	oc13b12	BCR2G	18.497	0.126	15.720	0.118	37.853	0.336	0.851	0.002	2.051	0.006
FCT sanidine	oc13d13	612	18.498	0.098	15.589	0.118	37.629	0.285	0.842	0.003	2.042	0.007
FCT sanidine	oc13d14	612	18.457	0.139	15.587	0.089	37.687	0.320	0.845	0.002	2.046	0.004
FCT sanidine	oc13d15	612	18.450	0.200	15.515	0.166	37.656	0.402	0.843	0.003	2.048	0.007

Table A5 Supplementary Data (continued): LA-MC-ICPMS lead isotope ratio values three feldspars from Souders and Sylvester (2010)

Sample	Analysis ID	Std	^{206}Pb / ^{204}Pb	std error (1-sigma)	^{207}Pb / ^{204}Pb	std error (1-sigma)	$^{208}Pb/^{204}Pb$	std error (1-sigma)	$^{207}Pb/^{206}Pb$	std error (1-sigma)	$^{208}Pb/^{206}Pb$	std error (1-sigma)
Fisk. Bytownite	no18b10	BCR2G	13.229	0.050	14.473	0.053	33.020	0.112	1.092	0.002	2.495	0.003
Fisk. Bytownite	no18b11	BCR2G	13.291	0.049	14.553	0.054	33.193	0.117	1.095	0.002	2.497	0.003
Fisk. Bytownite	no18b12	BCR2G	13.269	0.036	14.433	0.040	33.025	0.089	1.087	0.001	2.485	0.003
Fisk. Bytownite	oc04a10	BCR2G	13.227	0.172	14.493	0.152	33.082	0.361	1.092	0.002	2.498	0.005
Fisk. Bytownite	oc04a11	BCR2G	13.292	0.155	14.492	0.122	33.022	0.324	1.090	0.002	2.493	0.005
Fisk. Bytownite	oc04a12	BCR2G	13.268	0.149	14.515	0.113	33.263	0.302	1.094	0.002	2.507	0.004
Fisk. Bytownite	oc04a16	BCR2G	13.277	0.162	14.444	0.130	33.070	0.333	1.088	0.002	2.491	0.006
Fisk. Bytownite	oc04a17	BCR2G	13.269	0.146	14.464	0.110	33.093	0.291	1.091	0.002	2.509	0.004
Fisk. Bytownite	oc04b10	BCR2G	13.279	0.098	14.395	0.102	32.991	0.240	1.091	0.003	2.517	0.009
Fisk. Bytownite	oc04b11	BCR2G	13.169	0.081	14.386	0.080	33.092	0.204	1.092	0.003	2.519	0.008
Fisk. Bytownite	oc04b12	BCR2G	13.257	0.088	14.435	0.089	33.221	0.219	1.089	0.003	2.511	0.008
Fisk. Bytownite	oc04b16	BCR2G	13.329	0.095	14.544	0.094	33.234	0.230	1.091	0.004	2.495	0.010
Fisk. Bytownite	oc04b17	BCR2G	13.237	0.082	14.443	0.085	33.076	0.205	1.091	0.003	2.503	0.008
Fisk. Bytownite	oc12a04	BCR2G	13.225	0.082	14.478	0.075	32.983	0.166	1.094	0.002	2.496	0.004
Fisk. Bytownite	oc12a05	BCR2G	13.225	0.085	14.473	0.079	32.961	0.181	1.094	0.001	2.494	0.005
Fisk. Bytownite	oc12a06	BCR2G	13.323	0.080	14.523	0.072	33.114	0.171	1.090	0.001	2.498	0.005
Fisk. Bytownite	je29b06	BCR2G	13.262	0.116	14.470	0.100	32.933	0.230	1.091	0.002	2.496	0.006
Fisk. Bytownite	je29b10	BCR2G	13.319	0.109	14.538	0.100	33.116	0.220	1.091	0.002	2.501	0.006
Fisk. Bytownite	je29b11	BCR2G	13.260	0.101	14.468	0.102	33.033	0.221	1.091	0.003	2.499	0.006
Fisk. Bytownite	je29b12	BCR2G	13.293	0.115	14.492	0.131	33.010	0.267	1.090	0.002	2.489	0.006
Fisk. Bytownite	oc12b04	612	13.321	0.070	14.490	0.093	33.164	0.219	1.087	0.004	2.498	0.005
Fisk. Bytownite	oc12b05	612	13.264	0.066	14.517	0.091	33.224	0.212	1.094	0.004	2.497	0.005
Fisk. Bytownite	oc12b06	612	13.282	0.101	14.368	0.134	32.986	0.310	1.090	0.004	2.499	0.007

Table A6 Supplementary Data: LA-MC-ICPMS lead isotope ratios for three sulfide matrices (Souders and Sylvester, 2010)

Sample	Analysis ID	Std	^{206}Pb / ^{204}Pb	std error (1-sigma)	^{207}Pb / ^{204}Pb	std error (1-sigma)	$^{208}Pb/^{204}Pb$	std error (1-sigma)	$^{207}Pb/^{206}Pb$	std error (1-sigma)	$^{208}Pb/^{206}Pb$	std error (1-sigma)
PB-1	oc25d10	612	20.619	0.099	15.816	0.097	39.707	0.261	0.767	0.003	1.916	0.005
PB-1	oc25d11	612	20.573	0.123	15.828	0.114	39.589	0.256	0.769	0.003	1.923	0.006
PB-1	oc25d12	612	20.553	0.145	15.889	0.137	39.498	0.297	0.769	0.003	1.920	0.005
PB-1	ap06c04	612	20.519	0.173	15.770	0.140	39.451	0.351	0.765	0.003	1.917	0.005
PB-1	ap06c05	612	20.567	0.137	15.848	0.120	39.508	0.293	0.767	0.003	1.913	0.005
PB-1	ap06c06	612	20.639	0.122	15.850	0.094	39.511	0.246	0.768	0.003	1.925	0.005
PB-1	ap06c16	612	20.590	0.240	15.877	0.192	39.654	0.500	0.771	0.003	1.919	0.006
PB-1	ap06c17	612	20.579	0.164	15.789	0.137	39.329	0.328	0.768	0.003	1.916	0.006
PB-1	ap06c18	612	20.589	0.203	15.795	0.173	39.468	0.430	0.768	0.003	1.927	0.006
PB-1	ju06a10	612	20.591	0.160	15.810	0.131	39.491	0.362	0.769	0.003	1.922	0.006
PB-1	ju06a11	612	20.530	0.158	15.761	0.131	39.403	0.341	0.770	0.003	1.914	0.006
PB-1	ju06a12	612	20.546	0.212	15.786	0.173	39.561	0.412	0.767	0.003	1.917	0.006
PB-1	ju06a16	612	20.607	0.162	15.805	0.141	39.544	0.344	0.766	0.004	1.921	0.005
PB-1	ju06a17	612	20.523	0.133	15.796	0.124	39.286	0.294	0.769	0.003	1.915	0.005
PB-1	ju06a18	612	20.689	0.146	15.941	0.124	39.412	0.310	0.770	0.003	1.908	0.004
PB-1	ju06a22	612	20.571	0.206	15.929	0.172	39.564	0.410	0.773	0.003	1.927	0.006
PB-1	ju06a23	612	20.594	0.281	15.825	0.219	39.682	0.618	0.769	0.004	1.921	0.008
PB-1	ju06a24	612	20.581	0.188	15.978	0.143	39.372	0.361	0.773	0.003	1.922	0.006
PB-1	ju06a28	612	20.574	0.223	15.947	0.193	39.561	0.472	0.772	0.004	1.921	0.007
PB-1	ju06a29	612	20.530	0.198	15.801	0.171	39.442	0.408	0.771	0.003	1.913	0.006
PB-1	ju06a30	612	20.559	0.157	15.842	0.139	39.329	0.334	0.769	0.004	1.907	0.005
PB-1	ju10a10	612	20.591	0.175	15.839	0.137	39.529	0.363	0.768	0.003	1.924	0.007
PB-1	ju10a11	612	20.618	0.220	15.856	0.187	39.154	0.454	0.774	0.003	1.917	0.008
PB-1	ju10a12	612	20.580	0.168	15.860	0.129	39.477	0.356	0.772	0.003	1.920	0.008
PB-1	ju10a28	612	20.533	0.139	15.861	0.106	39.448	0.287	0.771	0.003	1.922	0.007
PB-1	ju10a29	612	20.603	0.160	15.937	0.133	39.654	0.357	0.772	0.003	1.917	0.008
PB-1	ju10a30	612	20.615	0.142	15.884	0.120	39.583	0.333	0.773	0.003	1.918	0.008
PB-1	oc25a04	PB-1	20.603	0.084	15.878	0.084	39.576	0.168	0.769	0.002	1.922	0.003
PB-1	oc25a05	PB-1	20.576	0.110	15.800	0.105	39.620	0.223	0.767	0.002	1.927	0.004
PB-1	oc25a06	PB-1	20.639	0.111	15.827	0.109	39.616	0.227	0.770	0.002	1.923	0.003
PB-1	ju06b04	PB-1	20.582	0.212	15.838	0.181	39.643	0.398	0.768	0.003	1.920	0.005
PB-1	ju06b05	PB-1	20.604	0.205	15.777	0.185	39.301	0.398	0.769	0.003	1.917	0.0051
PB-1	ju06b06	PB-1	20.594	0.230	15.891	0.196	39.440	0.423	0.768	0.003	1.914	0.0055
PB-1	ju06b10	PB-1	20.666	0.181	15.857	0.157	39.433	0.326	0.770	0.003	1.918	0.005
PB-1	ju06b11	PB-1	20.635	0.189	15.819	0.170	39.599	0.370	0.767	0.003	1.919	0.005
PB-1	ju06b12	PB-1	20.615	0.214	15.756	0.188	39.393	0.434	0.767	0.003	1.918	0.005
PB-1	ju06b13	PB-1	20.513	0.176	15.712	0.136	39.502	0.362	0.768	0.003	1.927	0.007
PB-1	ju06b14	PB-1	20.604	0.139	15.813	0.105	39.548	0.287	0.770	0.003	1.923	0.0064
PB-1	ju06b15	PB-1	20.558	0.117	15.847	0.107	39.601	0.273	0.772	0.003	1.930	0.007

Table A6 Supplementary Data (continued): LA-MC-ICPMS lead isotope ratios for three sulfide matrices (Souders and Sylvester, 2010)

Sample	Analysis ID	Std	^{206}Pb / ^{204}Pb	std error (1-sigma)	^{207}Pb / ^{204}Pb	std error (1-sigma)	$^{208}Pb/^{204}Pb$	std error (1-sigma)	$^{207}Pb/^{206}Pb$	std error (1-sigma)	$^{208}Pb/^{206}Pb$	std error (1-sigma)
B41	oc11g04	612	18.658	0.415	15.582	0.357	38.242	0.918	0.844	0.005	2.049	0.010
B41	oc11g05	612	18.607	0.143	15.644	0.115	38.125	0.287	0.846	0.003	2.053	0.009
B41	oc11g06	612	18.558	0.205	15.690	0.168	37.795	0.395	0.844	0.004	2.041	0.008
B41	oc25d16	612	18.581	0.162	15.775	0.152	38.111	0.352	0.848	0.003	2.051	0.005
B41	oc25d17	612	18.607	0.225	15.692	0.178	37.948	0.457	0.842	0.004	2.040	0.007
B41	oc25d18	612	18.520	0.178	15.685	0.174	37.987	0.404	0.842	0.003	2.046	0.005
B41	ap06c10	612	18.606	0.131	15.673	0.131	38.057	0.277	0.840	0.003	2.042	0.005
B41	ap06c11	612	18.628	0.142	15.569	0.125	37.979	0.295	0.839	0.003	2.048	0.007
B41	ap06c12	612	18.591	0.251	15.617	0.216	37.897	0.522	0.840	0.004	2.045	0.008
B41	ju06a34	612	18.663	0.178	15.678	0.165	38.044	0.401	0.843	0.004	2.045	0.006
B41	ju06a35	612	18.514	0.201	15.642	0.216	37.901	0.474	0.841	0.004	2.054	0.007
B41	ju06a36	612	18.614	0.211	15.643	0.188	38.065	0.305	0.840	0.003	2.046	0.007
B41	ju06a40	612	18.568	0.243	15.573	0.211	38.186	0.530	0.846	0.004	2.057	0.007
B41	ju06a41	612	18.637	0.209	15.614	0.189	38.094	0.467	0.844	0.004	2.042	0.007
B41	ju06a42	612	18.520	0.281	15.570	0.231	37.858	0.579	0.844	0.005	2.053	0.009
B41	ju06a46	612	18.539	0.182	15.647	0.162	38.092	0.367	0.843	0.004	2.051	0.006
B41	ju06a47	612	18.639	0.178	15.724	0.149	38.210	0.391	0.841	0.004	2.051	0.006
B41	ju06a48	612	18.571	0.211	15.735	0.193	38.146	0.477	0.841	0.005	2.052	0.006
B41	ju06a52	612	18.717	0.235	15.693	0.205	38.203	0.511	0.839	0.004	2.042	0.007
B41	ju06a53	612	18.626	0.211	15.722	0.171	38.063	0.449	0.839	0.004	2.044	0.007
B41	ju06a54	612	18.591	0.234	15.580	0.196	37.793	0.496	0.841	0.004	2.046	0.008
B41	ju10a16	612	18.525	0.221	15.631	0.173	38.014	0.441	0.845	0.003	2.055	0.009
B41	ju10a17	612	18.635	0.159	15.673	0.130	38.092	0.347	0.843	0.003	2.050	0.008
B41	ju10a34	612	18.602	0.202	15.647	0.174	38.119	0.423	0.842	0.004	2.043	0.008
B41	ju10a35	612	18.592	0.250	15.617	0.210	38.367	0.550	0.846	0.003	2.053	0.009
B41	ju10a36	612	18.569	0.171	15.552	0.159	37.827	0.392	0.844	0.004	2.044	0.009
B41	oc11h04	PB-1	18.621	0.145	15.647	0.180	38.068	0.372	0.838	0.004	2.046	0.0060
B41	oc11h05	PB-1	18.504	0.163	15.630	0.170	38.241	0.340	0.845	0.003	2.055	0.0062
B41	oc11h06	PB-1	18.587	0.182	15.645	0.177	38.122	0.405	0.841	0.003	2.053	0.0073
B41	oc25a10	PB-1	18.582	0.159	15.684	0.143	38.316	0.336	0.845	0.002	2.057	0.005
B41	oc25a11	PB-1	18.540	0.171	15.686	0.173	38.073	0.459	0.845	0.002	2.059	0.005
B41	oc25a12	PB-1	18.591	0.235	15.700	0.224	38.012	0.478	0.845	0.003	2.053	0.007
B41	ap06c25	PB-1	18.693	0.163	15.790	0.172	38.108	0.345	0.845	0.003	2.048	0.006
B41	ap06c26	PB-1	18.628	0.161	15.772	0.179	38.111	0.356	0.843	0.003	2.051	0.007
B41	ap06c27	PB-1	18.583	0.208	15.766	0.202	38.095	0.438	0.846	0.004	2.052	0.008
B41	ju06b19	PB-1	18.626	0.190	15.730	0.188	38.331	0.445	0.841	0.004	2.048	0.010
B41	ju06b20	PB-1	18.601	0.219	15.591	0.175	38.022	0.462	0.843	0.004	2.059	0.009
B41	ju06b26	PB-1	18.599	0.188	15.772	0.159	38.321	0.388	0.844	0.004	2.060	0.009
MASS-1	fe25e10	612	21.024	0.556	16.248	0.415	40.557	1.031	0.777	0.003	1.931	0.008
MASS-1	fe25e11	612	20.753	0.256	16.110	0.203	40.346	0.458	0.777	0.003	1.944	0.007
MASS-1	fe25e12	612	20.286	0.262	15.702	0.207	39.670	0.507	0.777	0.003	1.951	0.007
MASS-1	fe25e25	PB-1	20.034	0.324	15.548	0.237	39.080	0.603	0.776	0.003	1.950	0.006
MASS-1	fe25e26	PB-1	19.775	0.353	15.327	0.250	38.675	0.656	0.775	0.003	1.949	0.006
MASS-1	fe25e27	PB-1	21.582	0.382	16.766	0.283	42.261	0.721	0.776	0.003	1.949	0.006